Instrumentation of a Roller Compactor to Monitor Vibration Behavior during Earthwork Compaction

Robert V. Rinehart and Michael A. Mooney

***Abstract*— Among the goals of intelligent soil compaction is feedback control of vibration frequency, force amplitude, and forward velocity to optimize the compaction of soil. The development of a robust model structure for feedback control and/or soil parameter identification for continuous quality control/quality assurance requires comprehensive information about the machine's behavior, e.g., vibration characteristics. This paper describes the development of a comprehensive instrumentation system to monitor the three dimensional vibration of key roller compactor components. The measurement techniques are explained in detail, and experimental data is presented to demonstrate the nature of response observed during field testing.**

***Index Terms*— Intelligent Compaction, Vibration Monitoring, Accelerometers, Hall Effect Sensors**

I. Introduction

Intelligent soil compaction employs feedback control of vibration frequency, force amplitude, and forward velocity to optimize the compaction of soil and to prevent damaging over-compaction. The development of a robust model structure for feedback control and/or soil parameter identification for continuous quality control/quality assurance requires comprehensive information about the machine's behavior. In the case of vibration monitoring of soil compaction [1],[2], continuous information about the salient vibration characteristics of the roller during operation is critical to model development, parameter estimation, and intelligent soil compaction.

This paper describes the development and deployment of a comprehensive instrumentation system to monitor the vibration of a roller compactor. Specific issues addressed in this paper include the selection and placement of accelerometers to capture the three dimensional response of critical roller components, and the measurement of the rotating eccentric mass position within the drum to reproduce the input force time history. Experimental data is presented to explain the nature of vibration response observed and performance of the instrumentation.

R. V. Rinehart is a Ph.D. student, Civil Engineering Systems, Colorado School of Mines, Golden, CO 80401 (e-mail: rrinehar@mines.edu).

M. A. Mooney is an Associate Professor, Engineering Division, Colorado School of Mines, Golden, CO 80401 USA (email: mooney@mines.edu).

II. Instrumentation

The vibratory roller compactor instrumented for this investigation was an Ingersoll-Rand DD-138HFA double smooth drum roller (see Fig. 1). Moreover, the instrumentation design and operation are directly applicable to single drum and padded-foot rollers. The DD-138HFA has a machine mass of 13,752 kg and a drum mass of 2,638 kg. Each drum is 1.4 m in diameter and 2.1 m in length. Within each drum, an eccentric mass configuration rotating about the drum axle (see Fig. 2) provides the vibratory or eccentric force:

$$f_{ecc}(t) = m_0 e_0 \omega^2 \cos(\omega t) \quad (1)$$

where ω is the circular frequency (rad/s), m_0 is the eccentric mass, and e_0 is the eccentricity. The eccentric force amplitude is dependent on the product m_0e_0 and ω. The frequency of vibration ω or more commonly $f=\omega/2\pi$ is computer-controlled by the operator and varies from 0-70 Hz for low amplitude. The eccentric mass m_0e_0 has eight settings varying from approximately one kg-m to more than two kg-m, and must be changed manually (described below).

An overview of the instrumentation system is illustrated in Fig. 1. For explanation purposes, forward travel is shown in Fig. 1d, and would be considered to the right in Fig. 1a and to the left in Fig. 1e. Right side and left side of the machine are taken with respect to the operator as he/she is traveling in the forward direction. Drum and frame vibration was monitored in three-dimensions using accelerometers. As observed in Fig. 1, the drum-frame connection configuration is different on the right and left sides. As such, drum vibration was monitored on the right side only where there was access to a non-rotating mount (see Fig. 1d). Frame acceleration was monitored on both sides. The position of the rotating eccentric mass was monitored on the left side of each drum using Hall Effect (HE) sensors.

All data was acquired from the sensor via a 16-bit, 200-kHz data acquisition system (DAS). The DAS, manufactured by IOTech, Inc. (Cleveland OH, www.iotech.com) is equipped with an Ethernet port which provides continuous data streaming to a laptop PC onboard the roller compactor, and has 16 programmable input voltage ranges. The DAS uses a multiplexer to sample analog inputs from the sensors installed on the roller compactor and therefore signals are not

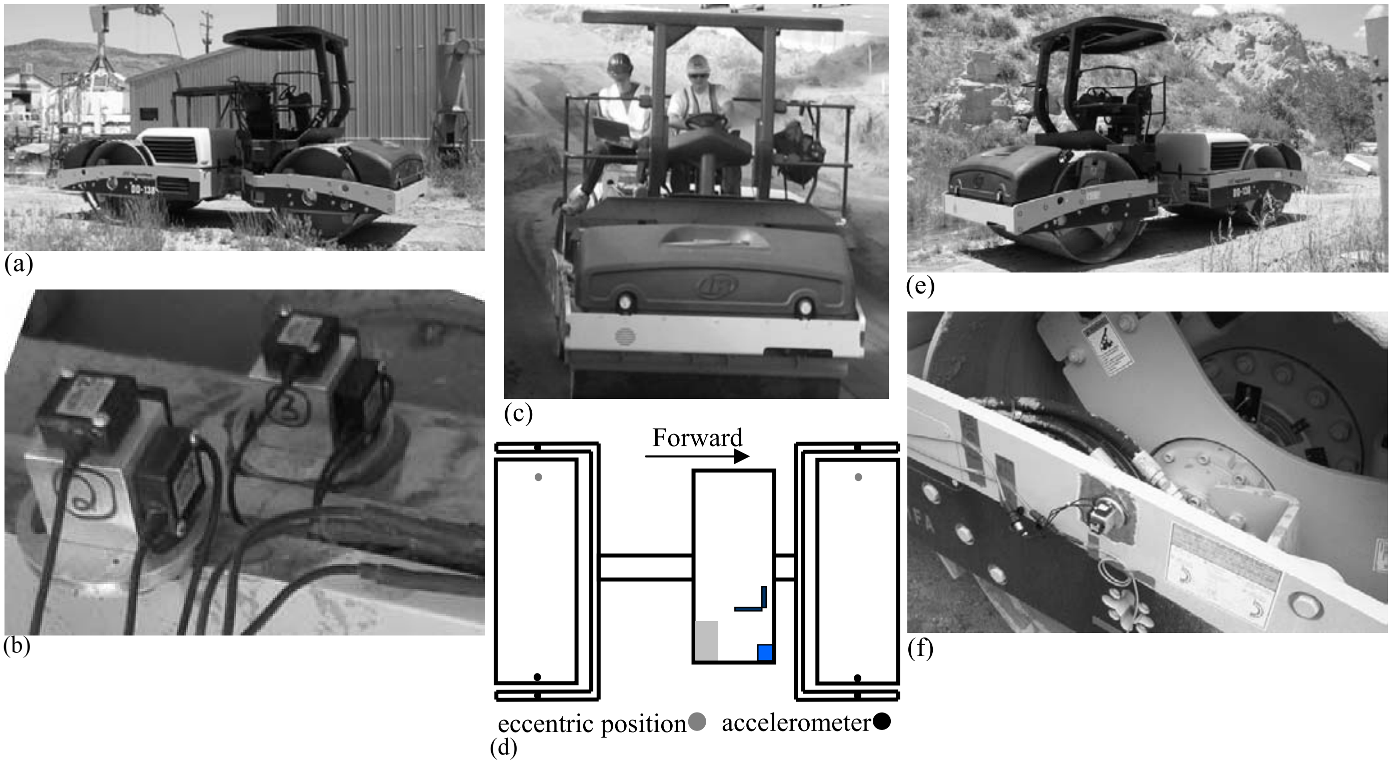

Fig. 1. (a) The Ingersoll-Rand DD138HFA roller compactor viewed from the right, (b) the drum and frame accelerometer mounts on the right side of the machine, (c) the roller compactor viewed from the front, (d) a plan view schematic summarizing all sensor locations, (e) the roller compactor viewed from the left, and (f) the frame accelerometer mounts on the left side of the machine, and the hand wheel used to adjust the vibration amplitude and monitor the position of the rotating eccentric mass.

sampled simultaneously. However, the delay between adjacent channels – 5 μs – is much less than the sampling frequency. Past research has shown that up to the fourth harmonic of the excitation frequency is of interest, and given that the maximum excitation frequency possible with the DD138 is 70Hz, the highest frequency of interest is 280 Hz [1]. The multiplex delay of 5 μs is 0.14% of one period of 280 Hz vibration and was therefore considered to be negligible.

Another important characteristic of the DAS is anti-aliasing. Anti-aliasing, in conjunction with an appropriate sampling frequency, fs, ensures that the wave form being acquired by the DAS does not have aliased components. In the case of this DAS anti-aliasing is achieved with a 3-pole Butterworth low pass filter (LPF). The filter has a hardware programmable cutoff frequency, f_{LPF}, which is set by varying a resistor-capacitor module in the hardware. An example configuration used in this study is f_{LPF} equal to 500 Hz and f_s equal to 2.5 kHz. Based on the Nyquist Sampling Theorem, this combination ensures that the sampled signal is free of aliased components, and that the highest frequency allowed to pass through the LPF is well resolved [3].

In addition to the accelerometers and HE sensors described below, the DAS captured operating frequency and forward velocity from the vehicle bus.

Vibration Monitoring

Due to asymmetry in the machine and the potential non-uniform soil conditions, each roller drum and its surrounding frame assembly will potentially experience six degree-of-freedom motion as illustrated in Fig. 2. To capture such

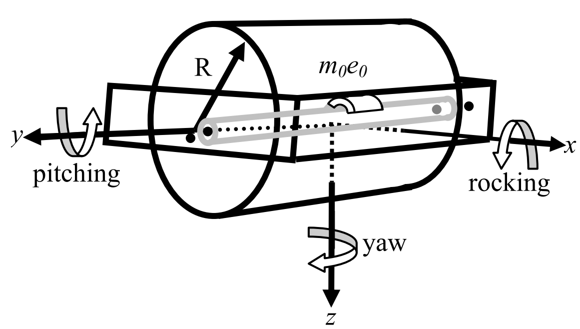

Fig. 2. Schematic of the front drum and frame showing axis orientation, six degree-of-freedom motion, and sensor locations.

Table I: Accelerometer Specifications

	Drum	Frame
Range	± 10 g	± 5 g
Sensitivity	200 mV/g	400 mV/g
Bandwidth	0-400 Hz	0-300 Hz
Non-linearity	0.5 % span	0.5 % span
Temperature Error (-20 to 85°C)	2.0 %	2.0 %
Transverse Sensitivity	1.0 % span	1.0 % span
Output Noise	0.5 mV p-p	0.5 mV p-p

motion, ICSensors triaxial translation accelerometers developed and manufactured by Measurement Specialties (Hampton VA, www.msiusa.com/icsensors/) were placed at the drum and frame locations shown in Fig. 2. The specifications of the ICSensors model 3140 accelerometers employed are summarized in Table I. The accelerometers used are piezoresistive type sensors. The sensing element is a micro-machined silicon mass suspended by multiple beams from a silicon frame. Piezoresistors located in the beams change their resistance as the motion of the suspended mass changes the strain in the beams.

The critical accelerometer specifications included range, sensitivity, noise floor, frequency response, nonlinearity, transverse sensitivity, and temperature error. Typical drum acceleration amplitudes observed during testing (x and z directions) range from ±0.5 g at 20 Hz vibration to ± 9 g at 70 Hz vibration. Due to the rubber mounts that connect each drum to its frame, frame acceleration amplitudes are typically 10-20% of the drum acceleration and hence can range in amplitude from ±0.05 g to ±2 g (x and z direction). Given this range and the need to accurately capture accelerations between peaks, a high sensitivity and low noise accelerometer was desired. For example, with a sensitivity of 200 mV/g and a noise of 0.5 mV p-p, the signal to noise ratio at a drum acceleration amplitude of ±0.5 g would be 400. A significant bandwidth was needed to capture both the 0 Hz (DC) response and vibration up to 300 Hz. The DC capability provides assistance during installation to ensure that the accelerometers are truly oriented in the x, y, and z directions, i.e., at 0 Hz on a horizontal surface the z acceleration should read 1 g. The high end of the bandwidth permits the capture of harmonics, i.e., multiples of the eccentric frequency, in the vibration response. Harmonic content provides a measure of system and soil nonlinearity; harmonic content as high as 300 Hz has been observed during vibratory compaction [1],[4].

Due to the large range of accelerations observed during testing, a high degree of linearity was required. And, due to the potential fluctuations in temperature on job sites, a low temperature-induced drift of the sensitivity was required. Temperature can very easily vary by 30 °C on a construction site during the day.

In order to quantify the sources of noise present in the instrumentation system, including the DAS, several studies were performed. One such study involved acquiring a signal from a stationary accelerometer using different methods to supply power to the sensor and the DAS. The results of this study revealed that a DC battery, such as a deep cycle marine battery, is a very clean power source and is preferable to a standard DC power supply. Powering the accelerometers and the DAS directly from a DC battery led to noise levels being controlled by the noise floor of the accelerometers themselves (see Table I), rather than external noise sources.

Other sources of noise include electronic interference from overhead or buried power lines and onboard electronics, seismic vibrations from other equipment operating on-site or nearby traffic, and unmonitored machine vibrations such as engine vibrations. Electronic interference was mitigated by ensuring that all elements within the instrumentation and the DAS were properly shielded with foil shielding. With the machine on a construction site, but turned off (and therefore stationary) several samples of accelerometer data were acquired. Analysis of these samples revealed that the noise floor (one standard deviation) under normal operation is approximately 10-15 mg.

Eccentric Force

Knowing the location of the rotating eccentric inside the drum allows for the calculation of the forcing function that the roller compactor inputs to the soil, as well as important machine-soil system parameters including the phase lag of drum displacement with respect to eccentric force. The amplitude adjustment hand wheel shown in Fig. 1f and in more detail in Fig. 3 is rigidly connected to the eccentric mass, and therefore its rotation outside the drum is directly related to the rotation of the eccentric inside the drum. Taking advantage of this machine characteristic enables the position of the eccentric to be monitored. To this end, 10 magnets were placed on the hand wheel itself, evenly spaced at 36°±1°. The HE sensor was mounted to a fixed bracket as shown in Fig. 3.

In order to translate the data from the HE sensor into the forcing function time history, it is necessary to be able to

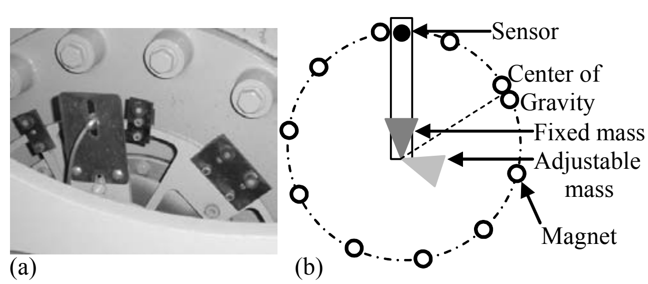

Fig. 3. (a) Amplitude adjustment hand wheel with magnets and Hall Effect sensor, and (b) sensor and magnet setup with adjustable eccentric mass and its center of gravity.

relate the relative location of the eccentric, as given by the pulses from the HE sensor, back to an absolute location (i.e. reference to 0^o). This was accomplished by making one of the magnet pulses twice as wide as the others. As shown in Fig. 3 the "double pulse" corresponds to the location of the eccentric mass's center of gravity which is known for each amplitude setting. The HE sensor outputs a high voltage (8.0 – 8.2 V) and is considered "on" when a magnet is sufficiently close and outputs a low voltage (0.0 – 0.2V), and is considered "off" when no magnet is detected. Due to sensor latency it is possible for a sample point to exist between fully off and fully on. Therefore the raw HE sensor data acquired by the DAS is *approximately* a square wave. For convenience and accuracy it is convolved with a thresholding function such that any sample point at or above 0.5 V is set to 1.0 and any sample point below 0.5 V is set to 0.0. This thresholding process is illustrated in Fig. 4.

Once the HE sensor data has been resolved into a perfect discrete square wave, it is possible to re-create the forcing function produced by the rotating eccentric mass. Using the 10 magnet pulses per revolution of the eccentric along with the knowledge of the position of the eccentric's center of gravity with respect to vertical (see Fig. 3b) the position of the eccentric can be determined at 10 locations per revolution. Given the rotational nature of the eccentric the forcing function will be of a sinusoidal form. Maximum eccentric force, see (1), occurs when the eccentric is in the downright position, whereas the eccentric force is zero when the eccentric is horizontal. Accordingly, as shown in Fig. 5, a sinusoid is fit to the series of known eccentric locations using a least squares approach. The results of this fit confirm that the forcing function is sinusoidal. However, due to hydraulic control of the eccentric mass, the frequency varies slightly with time (±0.25 Hz for 20 Hz vibration).

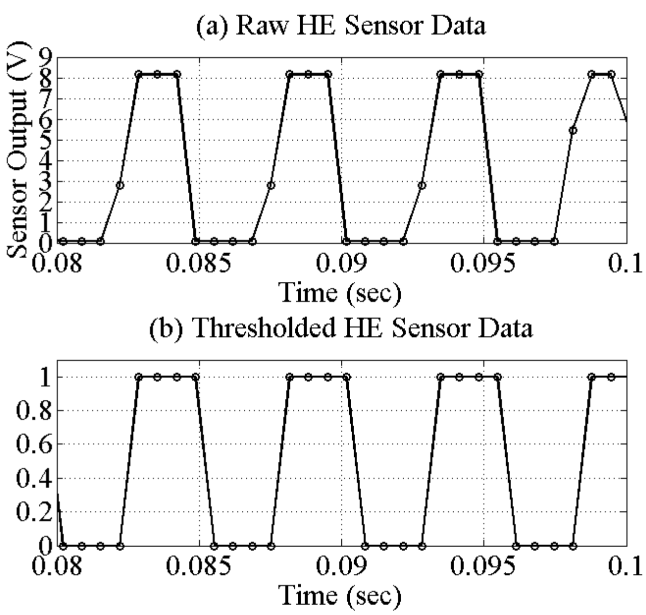

Fig. 4. (a) Raw Hall Effect sensor data, and (b) Hall Effect sensor data after being thresholded.

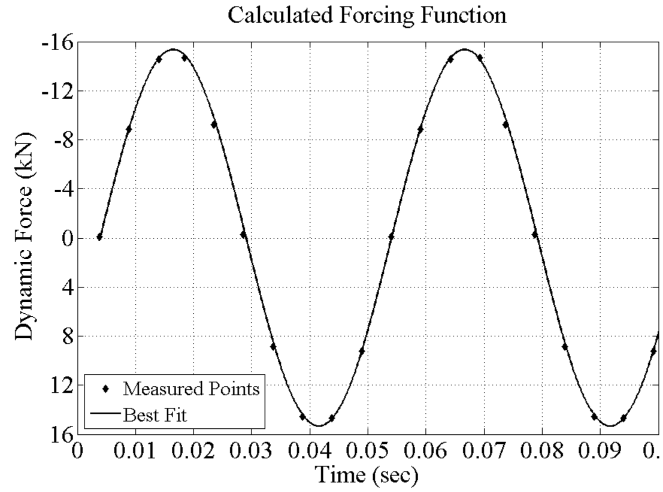

Fig. 5. The least squares best fit solution to the calculated forcing function data for two periods of eccentric rotation.

III. FIELD DATA REDUCTION

During operation and field testing, the instrumented roller travels at a constant forward (or reverse) velocity that can range from 0.5 to 3 m/s. Given the typical operating frequency range of 20-50 Hz and assuming a forward velocity of 1 m/s, a 1-m length of underlying soil will experience 20 to 50 cycles of vibratory loading. Fig. 6 presents some sample accelerometer data, specifically vertical drum acceleration collected at a sampling frequency of 1500 Hz during 20 Hz vibration (75 samples/cycle) and 2.0 m/s forward velocity. Given the positive down sign convention and knowing that acceleration and displacement are 180° out of phase, a positive drum acceleration peak occurs when the drum is in its highest position whereas a negative drum acceleration

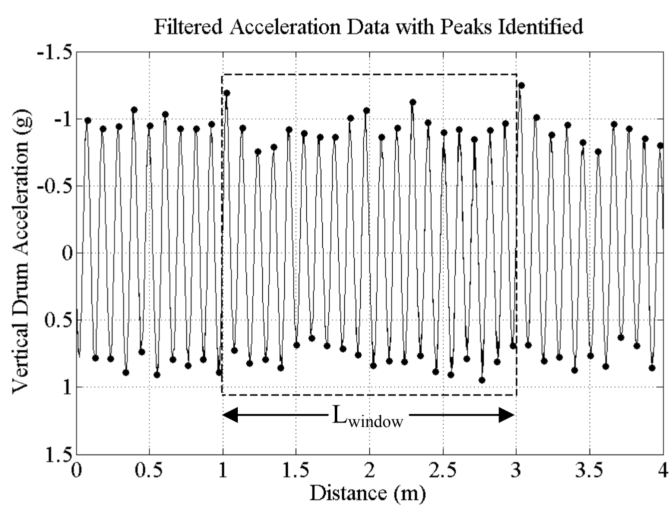

Fig. 6. Filtered vertical drum acceleration data with peaks identified, illustrating the averaging window used to smooth time domain acceleration data.

peak occurs when the drum is in its lowest position. Given the 0-300 Hz accelerometer bandwidth, higher frequency response is spurious noise and was filtered. The acceleration of gravity is subtracted from the vertical acceleration data. The fluctuation in acceleration response shown in Fig. 6 is much greater than the noise (10 mg as described in Section II), and is indicative of the traveling nature of the roller compactor and variation in underlying soil conditions. For time history analysis, peak values were gleaned from the data (filled circles in Fig. 6). A windowing approach to average acceleration peaks was then employed to smooth some fluctuations in response. The length of the window can vary; in Fig. 6, the window length is 2 m or 1.0 s.

Owing to the nonlinear nature of the coupled roller/soil system, the drum and frame acceleration response is not purely sinusoidal. The nonlinearity is manifested by the difference between peak positive and negative accelerations in Fig. 6, and by harmonic content in the frequency domain representation. To this end, displacement amplitudes as determined by $-a/\omega^2$ provide only an approximation of the true displacement. Fig. 7 illustrates the x, y, z front drum (right side) and front frame (right side) acceleration response determined over a broad range of operating frequencies. Fig. 7a illustrates the significant z drum displacement response, the somewhat lower x drum displacement response, and the fairly negligible y drum displacement response. The right side frame response (Fig. 7b) exhibits comparable x, y, and z displacements across the frequency domain, though due to the rubber isolators, much less than drum displacement. A closer evaluation of the data illustrates that the peak drum z response observed at 28 Hz is the resonant rocking mode. The resonant vertical drum translation mode occurs near 22 Hz.

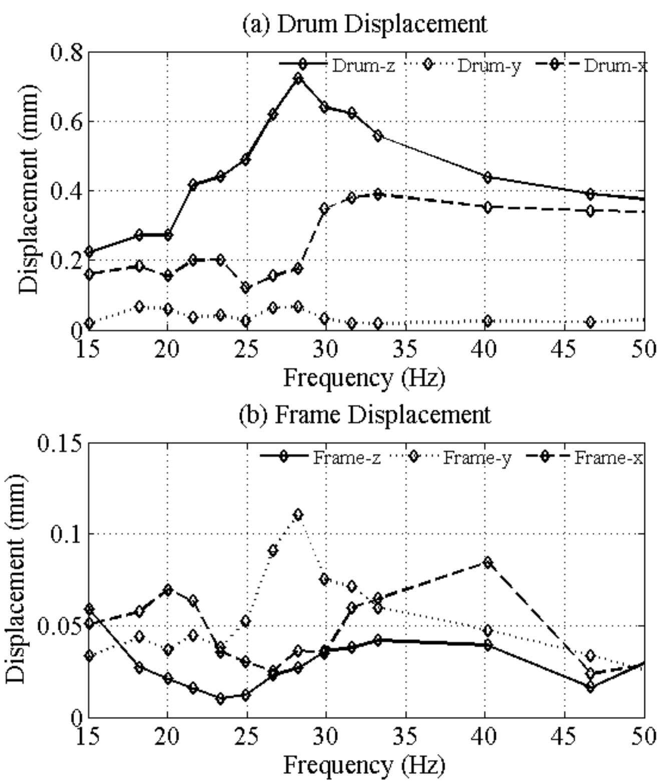

Fig. 7. (a) Drum displacement versus frequency, and (b) frame displacement versus frequency.

A sample of the vertical f_{ecc} time history is shown in Fig. 8 together with the front right vertical drum and frame displacement responses (approximated by $-a/\omega^2$). This response is representative of 30 Hz vibration which would be considered slightly above the natural z translation and rocking modes. The damped nature of the coupled system causes the drum displacement to be out of phase with the eccentric force. As illustrated in this particular sample set, the drum displacement lags the eccentric force by 126°. This phase lag is a function of the frequency ratio (operating frequency/natural frequency) and the damping ratio – both of which change during the compaction of soil – and thus is a very useful measure of changing soil properties.

If one were to model the roller compactor as a 2-dof lumped parameter system where the soil is represented by a linear spring and viscous damper [2],[5], the force transmitted to the soil f_{tr} would be determined as:

$$f_{tr}(t) = F_e \cos(\omega t) + (m_d + m_f)g - m_d \ddot{z}_d - m_f \ddot{z}_f \qquad (2)$$

where F_e is the force amplitude due to the eccentric ($m_0 e_0 \omega^2$), ω is the operating frequency, m_d and m_f are the mass of the drum and frame respectively, g is acceleration due to gravity, and $\ddot{z}_d$ and $\ddot{z}_f$ are the acceleration of the drum and frame respectively. If $f_{tr} > 0$, then the drum and soil are in contact; otherwise, if $f_{tr} < 0$, the drum is not in contact with the ground and is considered bouncing (undesirable from a machine wear

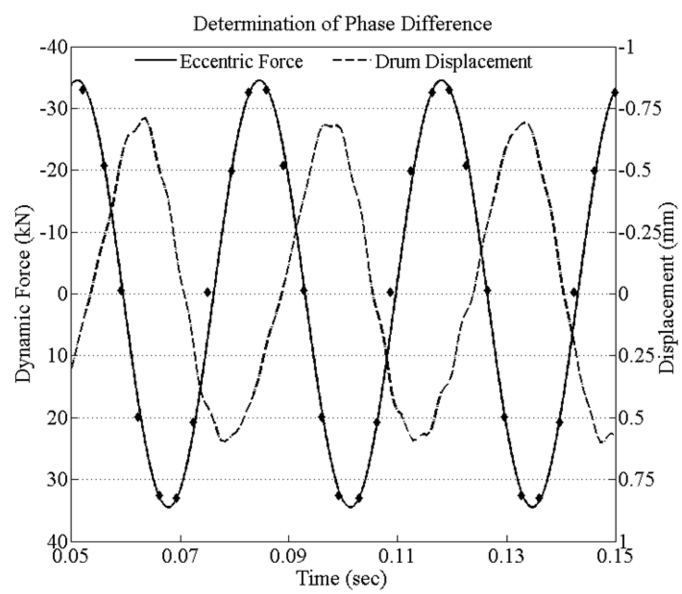

Fig. 8. Determining the phase difference between the dynamic force due to the eccentric and vertical drum displacement.

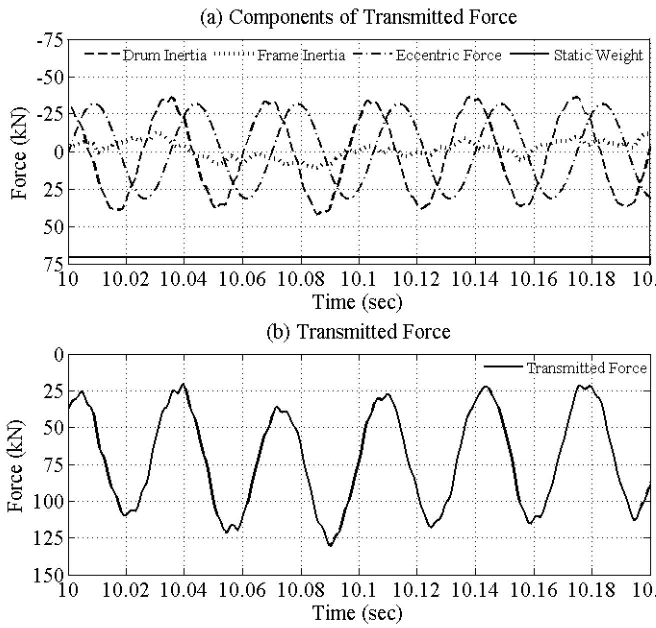

Fig. 9. Derivation of the force transmitted to the soil by the roller compactor from the rotating eccentric, drum and frame inertia forces, and the static weight of the machine.

perspective). Fig. 9 illustrates a segment of the four force components in (2) for a 30 Hz data set (positive force downward). As shown in Fig. 9, the static weight for the DD-138HFA is 70.65 kN and f_{ecc} oscillates between ± 35 kN. The drum inertia is significant, varying between 50 kN and -60 kN, and serves to counteract the eccentric force (though not 180° out of phase). The frame inertia is smaller than the other three forces. As a result, f_{tr} for this particular data set oscillates between 20 and 125 kN.

IV. Concluding Remarks

Realizing intelligent compaction wherein the machine parameters are adapted through feedback control to optimize the compaction process for all soils and stratigraphies is a complicated problem. Feedback control and system identification both require effective models of the coupled system, which in turn requires comprehensive continuous information about the machine's behavior. The instrumented roller compactor presented here provides comprehensive data regarding the machine's vibration characteristics and about the eccentric forcing function. This instrumentation system and subsequent data analysis has revealed translation and rocking mode vibration and phase lag behavior that are quite reflective of changes in underlying soil conditions.

References

[1] Mooney, M.A., Gorman, P.B. and Gonzalez, J.N. "Vibration Based Health Monitoring During Earthwork Construction," *Structural Health Monitoring*, 2005, Vol 2, No 4, 137-152.

[2] Anderegg, R and K. Kaufmann, Intelligent Compaction with Vibratory Rollers, Transportation Research Board Annual Meeting, Washington D.C., 2004.

[3] Lindler, D. K., *Introduction to Signals and Systems*. New York, NY: McGraw-Hill, 1999, pp.739-741.

[4] Mooney, M.A., Gorman, P.B., Chan, G.B. and Srour, C. "Observed Changes in Vibratory Roller Signature During Soil Compaction." Proc. 1st European Conf. on Structural Health Monitoring, 2002, Paris, France.

[5] Yoo, T.S. and Selig, T., "Dynamics of Vibratory-Roller Compaction," J. Geotechnical Engineering Division, ASCE, Vol., No. 1979, pp. 1211-1231.